

## Power Flow Control in HVDC-Link Using Artificial Neural Networks (ANN)

Dhanamjaya Apparao.A<sup>1\*</sup> S. Srikanth<sup>2\*</sup>

<sup>1\*</sup> Pursuing M.Tech, Department of Electrical and Electronics Engineering, B.V.C Engineering College, Odalarevu, Andhra Pradesh., India.

<sup>2\*</sup> Professor, Department of Electrical and Electronics Engineering, B.V.C Engineering College, Odalarevu, Andhra Pradesh.India.

**Abstract**— This paper describes the simulation of HVDC system which is used to transfer bulk amount of power between two converter stations. The main aim of this paper is to reduce the power loss in the HVDC system. In order to reduce these power losses, we go for power flow control. The power flow control can be done by controlling the rectifier and inverter stations with Artificial neural networks.

**Keywords**— HVDC Transmission, Simulation, Artificial neural networks, Conventional controller.

### I. INTRODUCTION

All of the early HVDC schemes were developed using mercury arc valves. The introduction of thyristor valves was demonstrated in 1972 with the first back-to-back asynchronous interconnection at the Eel River between Quebec and New Brunswick. Since then thyristor valve technology has completely replaced mercury arc valve technology. By 2008, a total transmission capacity of 100,000 MW HVDC has been installed in over 100 projects worldwide, more than 25,000 MW HVDC is under construction in 10 projects, and an additional 125,000 MW HVDC transmission capacity has been planned in 50 projects<sup>5</sup>. To account for the rapid growth of DC transmission and its technology it is necessary to include the HVDC transmission into the undergraduate power systems curriculum. Most undergraduate curriculum have only one course on power systems which is typically devoted to AC transmission systems. The Electrical and Computer Engineering program at York College of Pennsylvania has four concentration areas: power systems/energy conversion, embedded systems, signal processing/communication, and control systems. In accordance with operational requirements, flexibility and investment, HVDC transmission systems can be classified into two-terminal and multiterminal HVDC transmission systems. A monopolar link with ground return is usually employed in the HVDC submarine cable scheme, e.g. Konti-Skan, Fenno-Skan, Baltic cable and Kontek HVDC links. Instead of earth or sea return, a monopolar link with metallic return (low insulation) may be used. Although the DC-line investment and operational cost of monopolar link with metallic return are higher than those of monopolar link with ground return, due to no direct current flowing through earth during operations, transformer

magnetism saturation and electrochemistry corrosion can be avoided. Initially, Sweden-Poland Link was planned as a monopolar link with ground return. Finally owing to the environmental impact, Sweden-Poland Link became the first monopolar link with metallic return.

An HVDC transmission system consists of three basic parts:

- 1) A rectifier station to convert AC to DC
- 2) A DC transmission line and
- 3) An inverter station to convert DC back to AC.

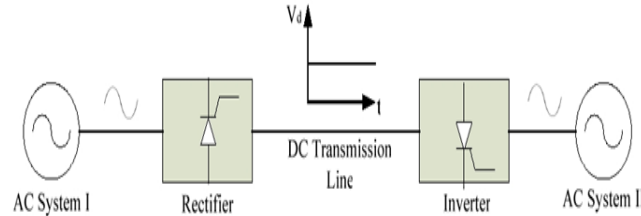


Fig 1. Schematic diagram of an HVDC transmission system

## II. HVDC SYSTEM MODEL

MATLAB/SIMULINK is a high-performance multifunctional software that uses functions for numerical computation system simulation, and application development.

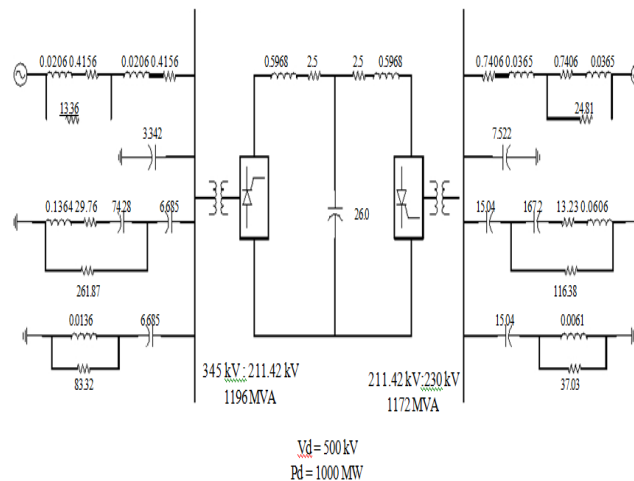


Fig 2. Schematic diagram of an HVDC transmission system

Power System Blockset (PSB) is one of its design tools for modelling and simulating electric power systems within the SIMULINK environment. It contains a block library with common components and devices found in electrical power networks that are based on electromagnetic and electromechanical equations. PSB/SIMULINK can be used for modelling and simulation of both power and control systems. PSB solves the system equations through state-variable analysis using either fixed or variable integration time-step. The linear dynamics of the system are expressed through continuous or discrete time-domain state-space equations. It also offers the flexibility of choosing from a variety of integration algorithms. The HVDC system shown in Fig.2. The system is a mono-polar 500-kV, 1000-MW HVDC link with 12-pulse converters on both rectifier and inverter sides, connected to weak ac systems (short circuit ratio of 2.5 at a rated frequency of 50 Hz) that provide a considerable degree of difficulty for dc controls. Damped filters and capacitive reactive compensation are also provided on both sides. The power circuit of the converter consists of the following subcircuits.

#### *A. AC Side*

The ac sides of the HVDC system consist of supply network, filters, and transformers on both sides of the converter. The ac supply network is represented by a Thevenin equivalent voltage source with an equivalent source impedance. AC filters are added to absorb the harmonics generated by the converter as well as to supply reactive power to the converter.

#### *B. DC Side*

The dc side of the converter consists of smoothing reactors for both rectifier and the inverter side. The dc transmission line is represented by an equivalent T network, which can be tuned to fundamental frequency to provide a difficult resonant condition for the modelled system.

#### *C. Converter*

The converter stations are represented by 12-pulse configuration with two six-pulse valves in series. In the actual converter, each valve is constructed with many thyristors in series. Each valve has a (di/dt) limiting inductor, and each thyristor has parallel RC snubbers.

#### *D. Power Circuit Modeling*

The rectifier and the inverter are 12-pulse converters constructed by two *universal bridge blocks* connected in series. The converter transformers are modeled by one three-phase two winding transformer with grounded Wye–Wye connection, the other by three-phase two winding transformer with grounded Wye–Delta connection. The converters are interconnected through a T-network.

##### *1) Universal Bridge Block:*

The universal bridge block implements a universal three-phase power converter that consists of six power switches connected as a bridge. The type of power switch and converter configuration can be selected from the dialog box. Series RC snubber circuits are connected in parallel with each switch device. The vector gating signals are six-pulse trains corresponding to the natural order of commutation. The and measurements are not realized in this model.

##### *2) Three Phase Source:*

A three-phase ac voltage source in series with a R-L combination is used to model the source.

##### *3) Converter Transformer Model:*

The three-phase two winding transformers models have been used where winding connection and winding parameters can be set through mask parameters. The tap position is at a fixed position determined by a multiplication factor applied on the primary nominal voltage of the converter transformers (1.01 on rectifier side; 0.989 on inverter side). The saturation has been simulated. The saturation characteristic has been specified by a series of current/flux pairs (in p.u.) starting with the pair (0,0).

### **III. CONTROL VARIABLES FOR CONSTANT POWER FLOW CONTROL**

The control model mainly consists of ( $\alpha/\gamma$ ) measurements and generation of firing signals for both the rectifier and inverter. The PLO is used to build the firing signals. The output signal of the PLO is a ramp, synchronized to the phase-A commutating.

Following are the controllers used in the control schemes:

1. Extinction Angle ( $\gamma$ ) Controller
2. dc Current Controller;
3. Voltage Dependent Current Limiter (VDCOL).

### 1) Rectifier Control:

The rectifier control system uses Constant Current Control (CCC) technique. The reference for current limit is obtained from the inverter side. This is done to ensure the protection of the converter in situations when inverter side does not have sufficient dc voltage support (due to a fault) or does not have sufficient load requirement (load rejection). The reference current used in rectifier control depends on the dc voltage available at the inverter side. Dc current on the rectifier side is measured using proper transducers and passed through necessary filters before they are compared to produce the error signal. The error signal is then passed through a PI controller, which produces the necessary firing angle order. The firing circuit uses this information to generate the equidistant pulses for the valves using the technique described earlier.

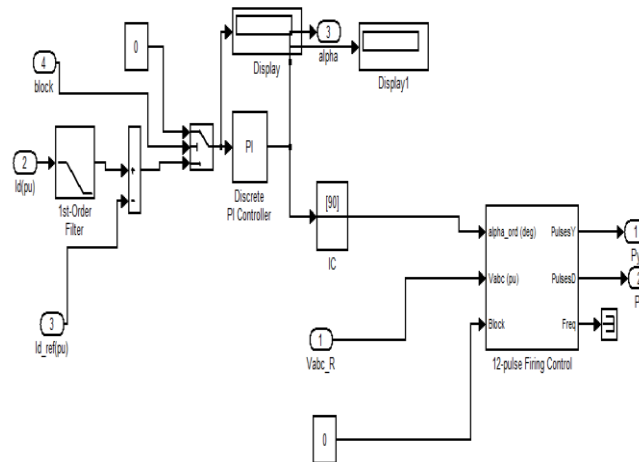


Fig 3. Rectifier control with PI.

### 2) Inverter Control:

The Extinction Angle Control or  $\gamma$  control and current control have been implemented on the inverter side. The CCC with Voltage Dependent Current Order Limiter (VDCOL) have been used here through PI controllers. The reference limit for the current control is obtained through a comparison of the external reference (selected by the operator or load requirement) and VDCOL (implemented through lookup table) output. The measured current is then subtracted from the reference limit to produce an error signal that is sent to the PI controller to produce the required angle order. The  $\gamma$  control uses another PI controller to produce gamma angle order for the inverter. The two angle orders are compared, and the minimum of the two is used to calculate the firing instant.

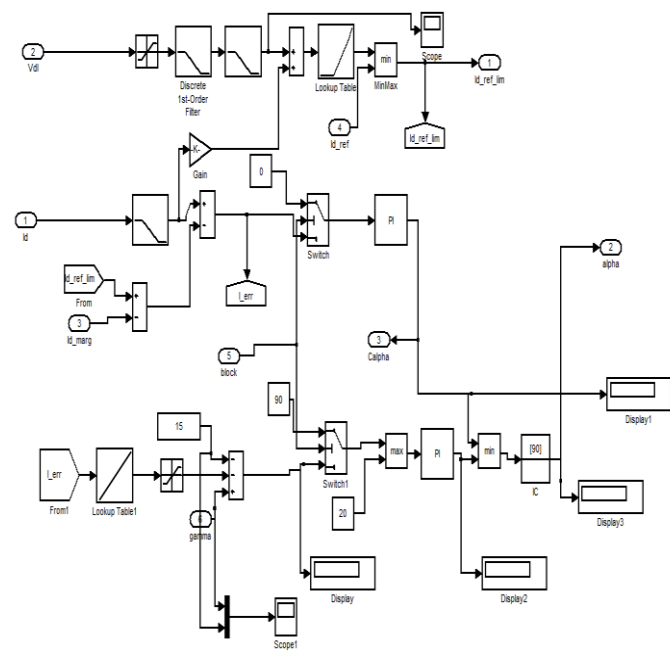


Fig 4. Inverter control with PI.

#### IV. SIMULATION RESULTS AND DISCUSSION

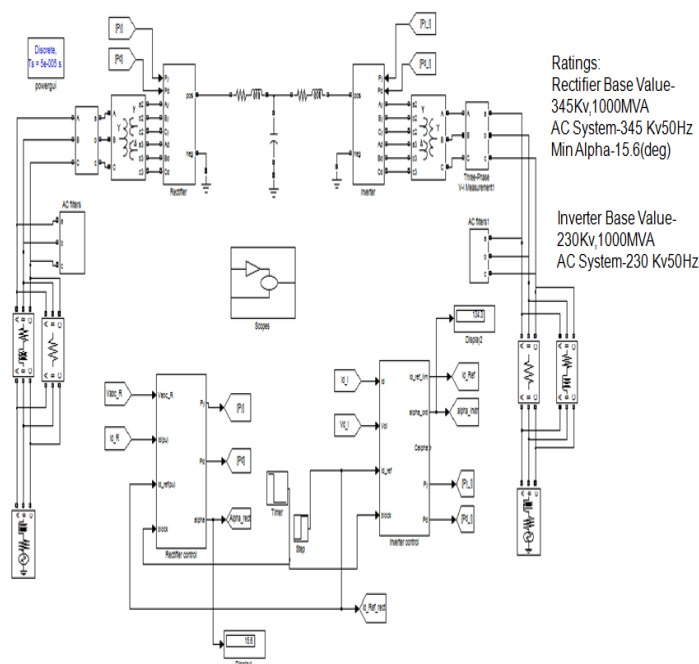


Fig 5. Simulink model of HVDC System

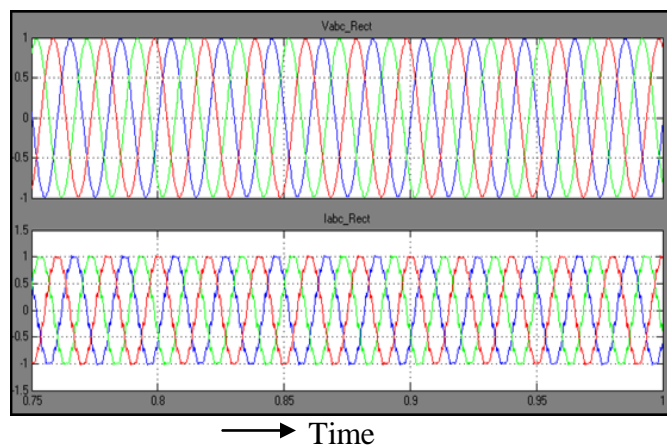


Fig 6. Rectifier side AC Voltage and AC Current

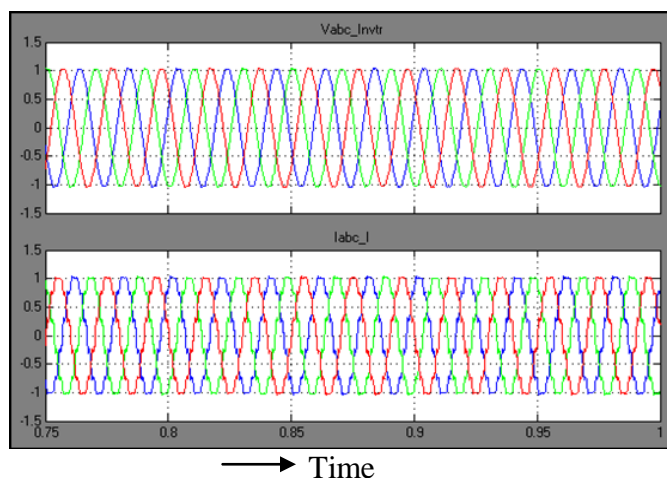


Fig 7. Inverter side AC Voltage and AC Current

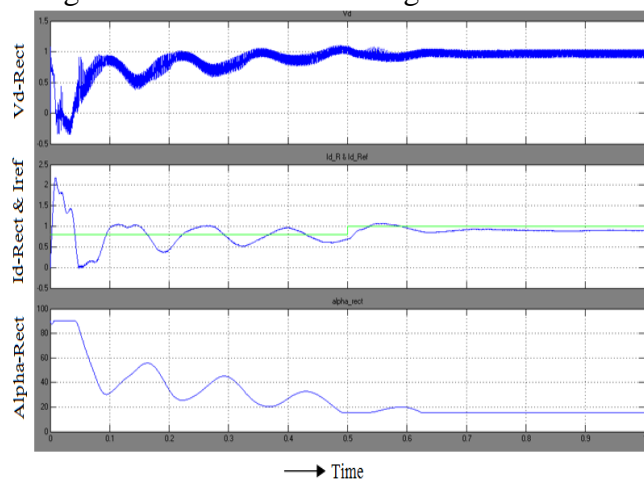


Fig 8. Rectifier side DC Voltage, DC Current and firing angle order with PI

From the above graph  $I_{d_R}$  and  $I_{d_{Ref}}$  are compared to produce an error signal which gives the firing angle order ( $\alpha=15.5$  deg).

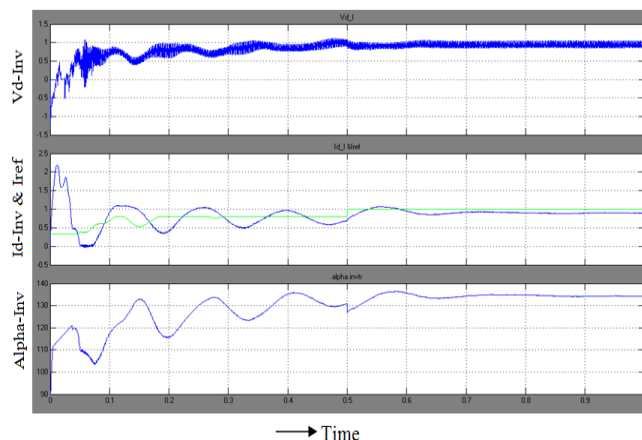


Fig 9. Inverter side DC Voltage, DC Current and firing angle order with PI

From the above graph  $I_{d\_I}$  and  $I_{d\_Ref}$  are compared to produce an error signal which gives the firing angle order ( $\alpha_{inv}=134$  deg).

## V. DESIGN OF ARTIFICIAL NEURAL NETWORKS

The fundamental processing element of a neural network is neurons. This building block of human awareness encompasses a few general capabilities. Basically, biological neurons receive inputs from other sources, combine them in some way, perform a generally nonlinear operation on the result, and then output the final result. Figure 7.1 shows the relationship of these four parts. Within humans there are many variations on this basic type of neurons, further complicating man's attempts at electrically replicating the process of thinking. Yet, all natural neurons have the same four basic Components.

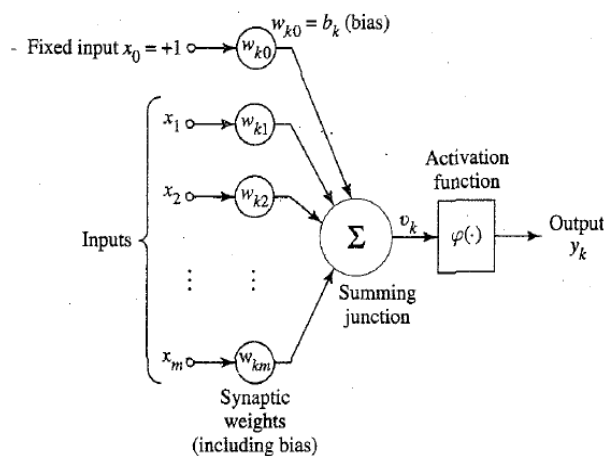


Fig10. Artificial Neural Networks

### 1) Supervised Training

In supervised training, both the inputs and the outputs are provided. The network then processes the inputs and compares its resulting outputs against the desired outputs. Errors are then propagated

back through the system, causing the system to adjust the weights are continually tweaked. The set of data which enables the training is called the “training set”.

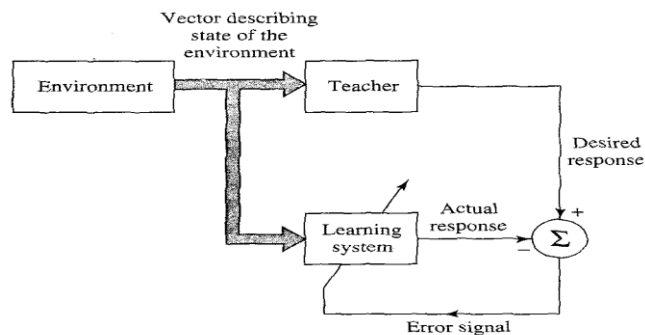


Fig11. Supervised training

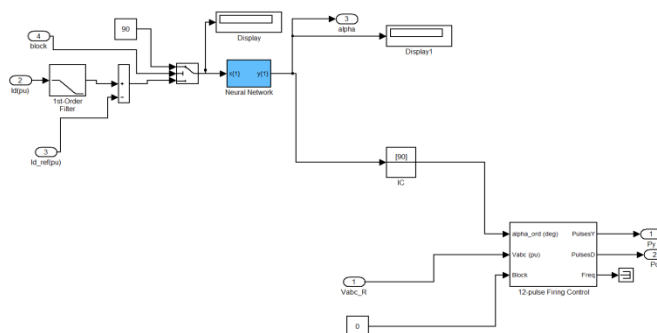


Fig 12. Rectifier control with ANN.

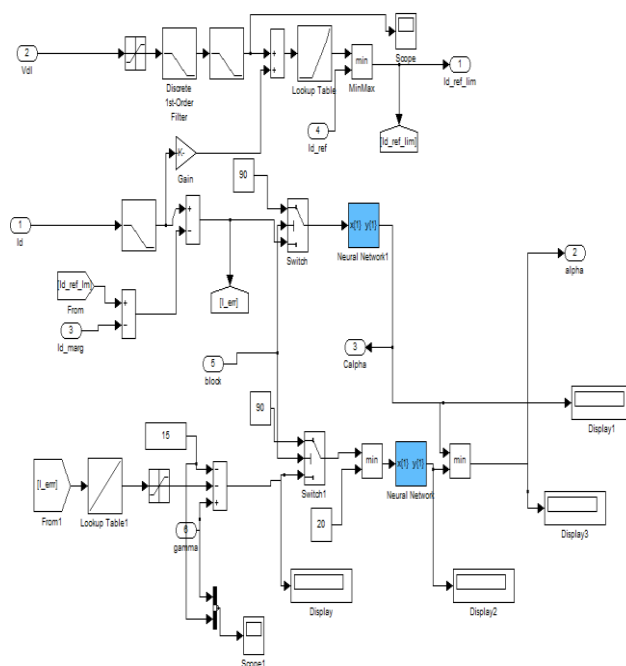


Fig 13. Inverter control with ANN



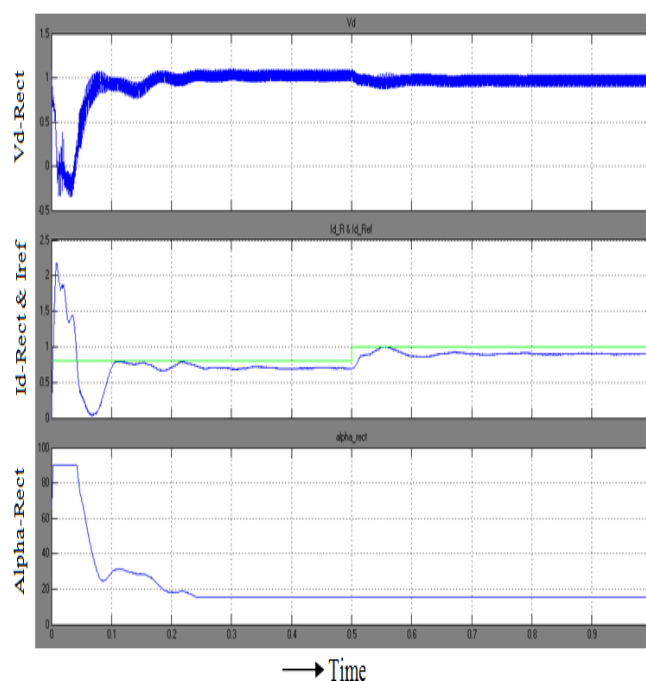


Fig 14. Rectifier side DC Voltage, DC Current and firing angle order with ANN

From the above graph  $I_{d\_R}$  and  $I_{d\_Ref}$  are compared to produce an error signal which gives the firing angle order ( $\alpha=15.5$  deg).

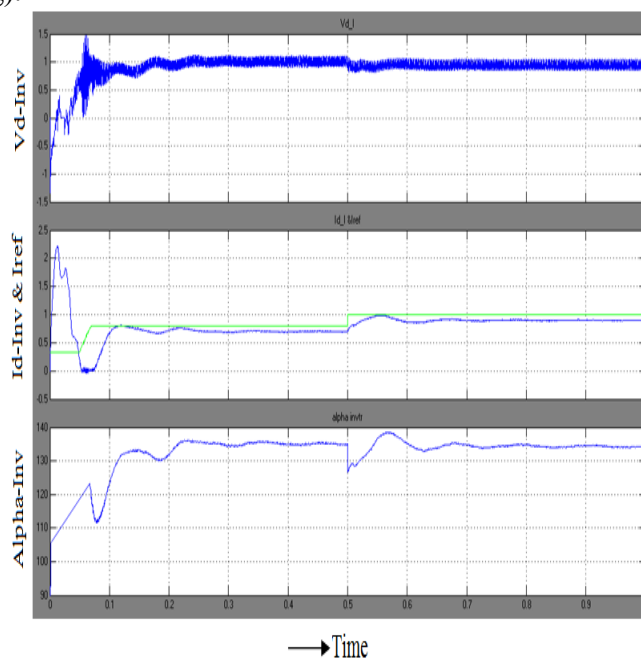


Fig 15. Inverter side DC Voltage, DC Current and firing angle order with ANN

From the above graph  $I_{d\_I}$  and  $I_{d\_Ref}$  are compared to produce an error signal which gives the firing angle order ( $\alpha_{inv}=142$  deg).

TABLE I  
EFFECT DUE TO CHANGE IN RECTIFIER FIRING ANGLE USING ANN

Rectifier $\alpha$ (degrees)	Inverter $\alpha$ (degrees)	$I_{d\_R}$ (p.u)	$I_{d\_I}$ (p.u)	$V_{d\_R}$ (p.u)	$V_{d\_I}$ (p.u)
15.5	142	0.903	0.9024	1.019	0.869
30	130	0.852	0.848	0.835	0.847
45	120.5	0.753	0.734	0.784	0.702
60	112	0.452	0.432	0.468	0.452
75	101	0.301	0.312	0.321	0.312

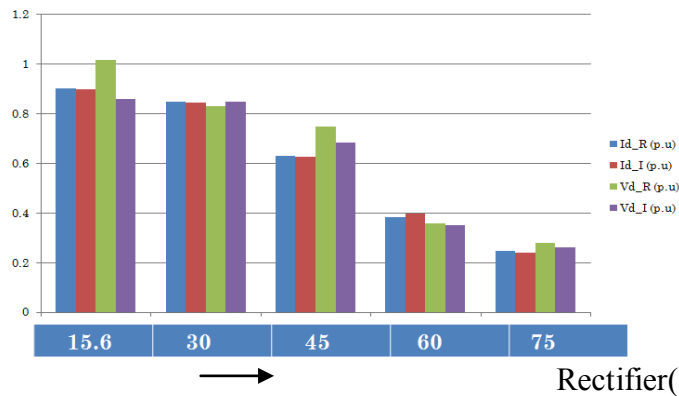


Fig 16. Effect due to change in Rectifier firing angle (chart representation) using ANN

## V1. CONCLUSION

In this paper, a HVDC system is designed to control the power flow between two converter stations with conventional controller and Artificial neural networks. The simulation results shows that the HVDC system with Artificial neural networks have better power flow control when compared with PI controller for different firing angles.

## APPENDIX I

### HVDC System Data

Parameters	Rectifier	Inverter
AC Voltage Base	345 kV	230 kV
Base MVA	1000 MVA	1000 MVA
Transformer taps (HV side)	1.01 p.u.	0.989 p.u.
Nominal DC Voltage	500 kV	500 kV
Nominal DC Current	2 kA	2 kA
Transformer $X_i$	0.18 p.u.	0.18 p.u.
Source Impedance	$R=0.4158\Omega, L=0.0206H$	$R=0.7406\Omega, L=0.0365H$
System Frequency	50 Hz	50 Hz
Nominal Angle	$\alpha=15^\circ$	$\gamma=15^\circ$

#### REFERENCES

- [1] M. O. Faruque, Yuyan Zhang and V. Dinavahi, "Detailed modeling of CIGRE HVDC benchmark system using PSCAD/EMTDC and PSB/SIMULINK," IEEE Trans. Power Delivery, vol.21, no.1, pp. 378 –387, Jan. 2006.
- [2] Das, B.P.; Watson, N.; Yonghe Liu; , "Simulation study of conventional and hybrid HVDC rectifier based on CIGRÉ benchmark model using PLL-less synchronisation scheme," Power Engineering and Optimization Conference (PEOCO), 2011 5th International , vol., no., pp.312-317, 6-7 June 2011doi: 10.1109/PEOCO.2011.5970433.
- [3] Ashfaq Thahir, M.; Kirthiga, M.V.; , "Investigations on modern self-defined controller for hybrid HVDC systems," TENCON 2011 - 2011 IEEE Region 10 Conference , vol., no., pp.938-943, 21-24 Nov. 2011doi: 10.1109/TENCON.2011.6129248.
- [4] Das, B.P.; Watson, N.; Yonghe Liu; , "Comparative study between gate firing units for CIGRE benchmark HVDC rectifier," Industrial Electronics and Applications (ICIEA), 2011 6th IEEE Conference on , vol.,no.,pp.299-306,21-23June2011 doi: 10.1109/ICIEA.2011.5975598.
- [5] Sood, V.K.; Khatri, V.; Jin, H.; , "EMTP modelling of CIGRE benchmark based HVDC transmission system operating with weak AC systems," Power Electronics, Drives and Energy Systems for Industrial Growth, 1996., Proceedings of the 1996 International Conference on , vol.1, no., pp.426-432 vol.1, 8-11 Jan 1996doi: 10.1109/PEDES.1996.539653.
- [6] Kala Meah, A.H.M. Sadrul Ula, "Simulation Study of the Frontier Line as a Multi-Terminal HVDC System," IEEE PES General Meeting, July 20- 24, 2008, Pittsburg, PA, USA.
- [7] N.G. Hingorani, "Power Electronics in Electronic Utilities: Role of Power Electronics in Future Power Systems," Proceeding of the IEEE, Vol. 76, No. 4, April, 1988, pp. 481-482.
- [8] A. Ekstrom and G. Liss, "A Refined HVDC Control System," IEEE Transactions on Power Apparatus and Systems, Vol. PAS-89, No. 5, May/June 1970, pp. 723-732.